New Sterically Stabilized Vesicles Based on Nonionic Surfactant, Cholesterol, and Poly(Ethylene Glycol)-Cholesterol Conjugates

Sophie Beugin,* Katarina Edwards,# Göran Karlsson,# Michel Ollivon,* and Sylviane Lesieur*
*Equipe Physico-Chimie des Systèmes Polyphasés, URA CNRS 1218, Université Paris-Sud, F-92296 Châtenay-Malabry, France, and #Department of Physical Chemistry, Uppsala University, S-75121 Uppsala, Sweden

ABSTRACT Monomethoxypoly(ethylene glycol) cholesteryl carbonates (M-PEG-Chol) with polymer chain molecular weights of 1000 (M-PEG1000-Chol) and 2000 (M-PEG2000-Chol) have been newly synthesized and characterized. Their aggregation behavior in mixture with diglycerol hexadecyl ether ($C_{16}G_2$) and cholesterol has been examined by cryotransmission electron microscopy, high-performance gel exclusion chromatography, and quasielastic light scattering. Nonaggregated, stable, unilamellar vesicles were obtained at low polymer levels with optimal shape and size homogeneity at cholesteryl conjugate/lipids ratios of 10 mol% M-PEG1000-Chol or 5 mol% M-PEG2000-Chol, corresponding to the theoretically predicted brush conformational state of the PEG chains. At 20 mol% M-PEG1000-Chol or 10 mol% M-PEG2000-Chol, the saturation threshold of the $C_{16}G_2$/cholesterol membrane in polymer is exceeded, and open disk-shaped aggregates are seen in coexistence with closed vesicles. Higher levels up to 30 mol% lead to the complete solubilization of the vesicles into disk-like structures of decreasing size with increasing PEG content. This study underlines the bivalent role of M-PEG-Chol derivatives: while behaving as solubilizing surfactants, they provide an efficient steric barrier, preventing the vesicles from aggregation and fusion over a period of at least 2 weeks.

INTRODUCTION

For the past 20 years, synthetic polyglycerol *n*-alkyl ethers or esters capable of combining with high amounts of cholesterol have proved to form biocompatible vesicular structures that are chemically and physically stable, characterized by a reduced membrane permeability to lipid- or water-soluble solutes (Vanlerberghe et al., 1978; Handjani-Vila et al., 1979, 1982; Uchegbu and Florence, 1995). These nonionic surfactant vesicles (NSVs), originally named "niosomes" (Vanlerberghe et al., 1978), have been worthily promoted to potential alternatives to liposomal delivery systems (Florence and Baillie, 1989). Most studies have indeed shown that NSVs prolong the circulation of entrapped drugs (Uchegbu and Florence, 1995; Azmin et al., 1985, 1986; Baillie et al., 1986; Hunter et al., 1988; Carter et al., 1988; Rogerson et al., 1987, 1988; Kerr et al., 1988; Raja Naresh and Udupa, 1996) or diagnostic markers (Erdogan et al., 1996). On the other hand, very little information focusing on the metabolism of NSVs themselves upon intravenous administration has been reported. It would seem, however, that to date, NSVs do not exhibit noticeably long circulation times in the bloodstream and thus behave in vivo like conventional phospholipidic vesicles (Azmin et al., 1985; Woodle and Lasic, 1992). In this respect, it has been widely demonstrated that the incorporation into the vesicle bilayer of glycolipids like monosialoganglioside GM_1 (Allen, 1992, 1994a; Allen and Papahadjopoulos, 1993; Oku and Namba, 1994), or of lipids derivatized with hydrophilic polymers, like polysaccharides (Akiyoshi and Sunamoto, 1992; Sato and Sunamoto, 1993) or, preferentially, poly(ethylene glycol) (PEG) (Woodle and Lasic, 1992; Allen, 1992, 1994a; Allen and Papahadjopoulos, 1993; Oku and Namba, 1994; Lasic and Needham, 1995; Woodle, 1993, 1995; Trubetskoy and Torchilin, 1995; Torchilin and Trubetskoy, 1995), significantly delays recognition and uptake by the cells of the reticuloendothelial system. The particular efficiency of surface-attached PEG chains has been explained by the combination of their water solubility and flexibility, which sterically stabilizes the vesicles, mainly preventing them from self-aggregation and/or fusion processes, as well as from opsonin adsorption (Needham et al., 1992; Lasic, 1994; Torchilin, 1996). Grafting PEG onto lipids through covalent bonding presents certain advantages. According to the chemical reactivity of the terminal hydroxyl groups, numerous compounds can be envisaged with characteristics befitting the host vesicle membrane. For instance, the lipid to be modified can be chosen from among the constituents of the initial lipid bilayer, and the chain length of the polymer moieties can be adjusted with regard to the wide range of available PEG molecular weights. The nature of the linkage between the PEG chain and the hydrophobic anchor can also be varied (Woodle and Lasic, 1992). Finally, the possible heterobifunctionalization of PEG allows subsequent attachment of biologically active or even cell-targeting molecules to the far end of the grafted polymer chain (Allen, 1994b, 1995; Blume et al., 1993).

The purpose of the present work is to introduce into the NSV membrane PEGylated additives exerting steric stabilization while preserving the original properties of the bilayer. Within the last 6 years, we have been especially

Received for publication 17 June 1997 and in final form 23 March 1998.
Address reprint requests to Dr. Sylviane Leiseur, Equipe Physico-Chimie des Systèmes Polyphasés, URA CNRS 1218, Université Paris-Sud, 5 rue J.-B. Clément, F-92296 Châtenay-Malabry, France. Tel.: 33-1-46-83-53-49; Fax: 33-1-46-83-53-12; E-mail: slesieur@cep.u-psud.fr.

0006-3495/98/06/3198/13 $2.00

interested in the physical characteristics and impermeability properties of NSVs composed of diglycerol hexadecyl ether ($C_{16}G_2$), cholesterol, and a small proportion of dicetylphosphate (DCP). These vesicles have revealed remarkable stability with time and strong resistance to solubilizing surfactants like octyl glucoside (Lesieur et al., 1990; Seras et al., 1992, 1993, 1994, 1996; Seras-Cansell et al., 1996) or Triton X-100 (Vanlerberghe and Morançais, 1996). Interestingly, these properties are connected to the condensing effect of cholesterol, present in nearly equimolar proportions with $C_{16}G_2$ (Vanlerberghe et al., 1978). Indeed, cholesterol is well known to confer cohesion on lipid bilayers by inducing tighter molecular packing and restricted motions of the hydrocarbon chains (Sankaram and Thompson, 1990; McMullen and McElhaney, 1996). The incorporation of DCP undoubtedly contributes to the stabilization of NSV dispersions (Seras et al., 1992; Florence, 1993). However, if the presence of a net electrical charge at the surface of the vesicles impedes their aggregation by creating repulsive forces, it inversely enhances their sensitivity to electrolytes, which can strongly limit the field of their biological applications. The use of nonionic amphipathic polymers then appears preferable, as a way to avoid this drawback. This is the main reason, in the following report, our choice has consisted of replacing the negatively charged compound DCP and a part of cholesterol molecules with PEG-grafted cholesterol while conserving the equimolarity between $C_{16}G_2$ and cholesteryl anchors. PEGylated cholesterol seemed quite appropriate, all the more so as recent investigations have shown that PEG cholesteryl ether (Uchegbu et al., 1992; Uchegbu and Florence, 1995) or sebacate diester (Chopineau et al., 1994) can be introduced at low levels in these vesicles while preserving the lamellar arrangement of the lipids assemblies. Moreover, the ability of PEG cholesteryl ether to prolong circulation half-lives of liposomes in vivo has also been stated (Allen et al., 1991; Ishiwata et al., 1995; Vertut-Doï et al., 1996), showing even better efficiency than PEG-distearoylphosphatidylethanolamine (PEG-DSPE), which is usually employed (Vertut-Doï et al., 1996; Schneider et al., 1996). It could be anticipated that choosing one constituent of NSVs as the PEG hydrophobic anchor, i.e., cholesterol, was specially suitable for minimizing the structural perturbations of the host bilayer upon incorporation of PEG additive. The structural characteristics of the resulting colloidal dispersions were examined as a function of both polymer content and length. The evolution of the aggregate morphology with the polyoxyethylene chain grafting density was discussed in terms of phase behavior of the lipid-polymer mixtures. The implication of the PEG chain conformation in this behavior was examined on the basis of a theoretical approach.

MATERIALS AND METHODS

Chemicals

Cholesterol and *n*-octyl-β-D-glucopyranoside (octyl glucoside, OG, purity >98%, M = 292.4) were purchased from Sigma. Dicetyl phosphate (DCP, purity = 97%, M = 546.9) and diglycerol hexadecyl ether (linear isomer C_{16H33}-(O-CH_2-CH(OH)-CH_2)$_2$-OH, $C_{16}G_2$, purity = 99% (Lesieur et al., 1990), M = 390) were supplied by L'Oréal (Chevilly-Larue, France). Cholesteryl chloroformate (CholCl, purity >99%, M = 449.12) and tetrabutylammonium chloride ($Bu_4N^+Cl^-$, purity >97%, M = 277.92) were purchased from Fluka. Monomethoxypoly(ethylene glycol) (M-PEG) with molecular weights of 1000 and 2000 (M-PEG1000 and M-PEG2000, respectively), characterized by a very low polydispersity index close to 1.05 according to the supplier, were from Shearwater Polymers Europe; their monomethyl functionality was confirmed by ^{1}H NMR. The buffer consisted of a 10 mM HEPES (Sigma) and 145 mM NaCl aqueous solution adjusted to pH 7.4 with 1 M NaOH.

Synthesis and purification of monomethoxypoly(ethylene glycol) cholesteryl carbonate

Monomethoxypoly(ethylene glycol) cholesteryl carbonate (M-PEG-Chol) has been synthesized in one step by the reaction of M-PEG on CholCl, using moderate phase transfer catalysis conditions previously described for the nucleophilic substitution of poly(vinyl chloroformate) by phenol (Boivin et al., 1983, 1985, 1988). In a typical experiment, 2.5 mmol of polymer dissolved in 10 ml CH_2Cl_2 was added dropwise to a magnetically stirred mixture containing 2.5 mmol of CholCl in 20 ml CH_2Cl_2, 0.125 mmol of $Bu_4N^+Cl^-$ (5 mol% of each reagent), and 3.75 mmol of NaOH in water (33 weight %) as HCl scavenger. The reaction scheme was as follows:

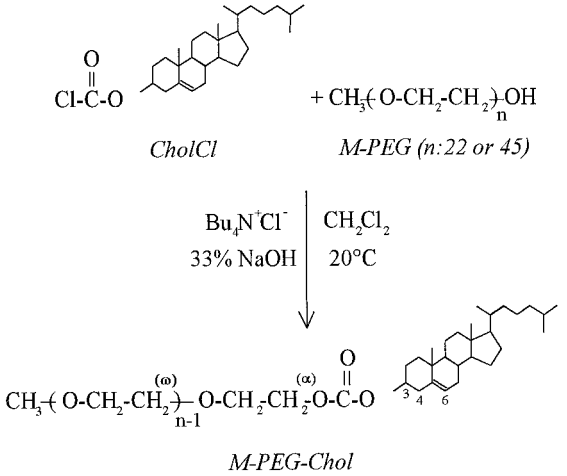

M-PEG-Chol

The reaction was carried out at room temperature, under nitrogen and continuous stirring. The formation of the M-PEG carbonate derivative was followed by thin-layer chromatography (plates RP-18, Merck; EtOH-CH_2Cl_2, 88:12, v/v) and infrared spectroscopy performed in CH_2Cl_2 with a Perkin-Elmer 782 apparatus. Substitution of chlorine in CholCl by M-PEG leads to the shift of the carbonyl absorption band from 1775 cm^{-1} to 1745 cm^{-1} (Fig. 1, *spectra b–d*), resulting from the change in the electronegativity of the neighboring α-atom of the carbonyl group (Boivin et al., 1983). The reaction was stopped after 7 days. The mixture was filtered to remove NaCl, and CH_2Cl_2 was evaporated under reduced pressure. The solid residue was suspended in 3 ml of ethyl acetate and deposited on the top of a 3 × 40 cm silica gel column. Unreacted CholCl and cholesterol formed by side hydrolysis of a small proportion of chloroformate molecules were first separated, using ethyl acetate as eluant. M-PEG-Chol and the remaining M-PEG were then recovered with EtOH-CH_2Cl_2, 9:91. The separation of M-PEG-Chol from M-PEG was performed by reverse-phase high-performance liquid chromatography (HPLC) on a 10.5 mm × 25 cm RSIL-C18HL preparative column (porosity, 10 μm; Touzart et Matignon) with methanol (HPLC grade; Prolabo) as the mobile phase (flow rate, 1 ml/min). The chromatograms obtained were similar to the one in Fig. 2. Methanol was rotavapped from the fraction containing

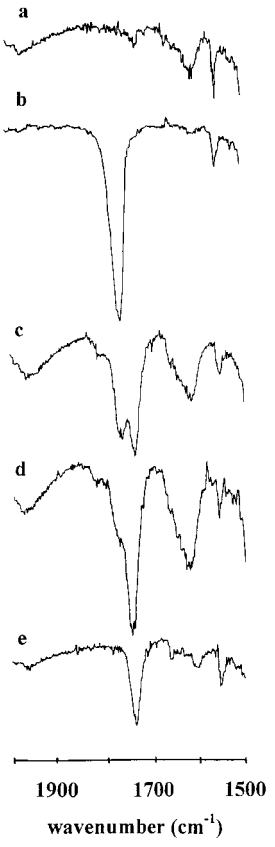

FIGURE 1 Infrared spectra of M-PEG (*a*) and CholCl (*b*) in CH_2Cl_2, organic phase formed during M-PEG2000-Chol synthesis at 3 days (*c*) and 7 days (*d*), 20 mM purified M-PEG2000-Chol in CH_2Cl_2 (*e*). The substitution of chlorine atoms in CholCl by M-PEG moieties is depicted by the shift of the carbonyl band from 1775 cm^{-1} to 1745 cm^{-1}.

M-PEG-Chol, which was then dried overnight under high vacuum and then stored at −20°C before use. Reaction yields after purification steps were found to be close to 30%.

The purity of M-PEG-Chol was checked by reverse-phase HPLC and infrared absorption analysis, particularly in the 1900–1500 cm^{-1} wavenumber range (Fig. 1, *spectrum e*). Regarding this, the band at 1615 cm^{-1} noticed for the initial M-PEG (Fig. 1, *spectrum a*), very likely due to unsaturated contaminants (Nadeau, 1967), was still observable for the nonpurified intermediate reaction mixtures (Fig. 1, *spectra c, d*), but had totally vanished after the purification procedure; only the carbonyl band at 1745 cm^{-1} characteristic of the carbonate group was recovered (Fig. 1, *spectrum e*). The purity of the polymer derivative was confirmed by ^1H NMR performed in $CDCl_3$ at 20°C with a 400 MHz Brüker instrument. The principal proton chemical shifts were (in ppm) (see reaction scheme for assignments): 5.35 (m, cholesteryl C(6)-H, ^1H), 4.43 (m, cholesteryl C(3)-H, ^1H), 4.23 (t, PEG CH(α)$_2$, 2H), 3.78–3.42 (PEG CH(ω)$_2$, (4n-4)H), 3.34 (s, PEG O-CH_3, 3H), 2.35 (m, cholesteryl C(4)-H_2, 2H), 1.99–0.64 (other cholesteryl H, 41H). Ratios of experimental integrations of signals located at 4.23 ppm (related to PEG moiety) and at either 4.43 ppm (related to cholesteryl moiety) or 3.34 ppm (methoxy group of PEG) ensured that each PEG chain is terminated at one end by one cholesteryl group and at the second end by one methoxy group.

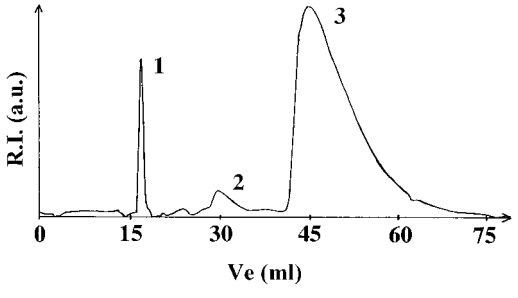

FIGURE 2 Preparative HPLC of M-PEG2000-Chol derivative in reverse-phase conditions on C_{18} alkylsilica (eluant, methanol; flow rate, 1 ml/min; refractive index detection): *1*, solvent front; *2*, remaining M-PEG; *3*, M-PEG-Chol derivative.

Mixed aggregates preparation

Nonionic surfactant vesicles based on $C_{16}G_2$, cholesterol, and DCP (48.0/48.4/3.6 mol%) were prepared by ultrasonic irradiation according to a procedure already detailed (Lesieur et al., 1990). M-PEG-coated particles were formed similarly. Chloroformic solutions of $C_{16}G_2$, cholesterol, and M-PEG-Chol (50/50-*x*/*x* mol%, $x = 2, 5, 10, 20, 30$) were evaporated under a gentle stream of nitrogen to obtain thin mixed lipid films (total lipid = 15 μmol). Residual organic solvent was eliminated by lyophilization. The films were hydrated with 3 ml buffer and vortexed. The lipid dispersions were maintained at 60°C for 4 h in hermetically closed flasks and alternately vortexed until complete homogenization. The milky suspensions were then ultrasonicated at 20°C for 6 × 2 min at power level 1.5, using a Vibracell Sonifier titanium probe (Sonics and Materials Corporation). The samples were finally centrifuged for 10 min at 10,000 rev./min to remove titanium particles of the ultrasonifier probe and filtered through a 0.22-μm Millex filter. Preparations were stored at room temperature.

Surface tension measurement

Surface tensions were measured with a Sanborn tensiometer. All experiments were performed at 23°C under saturated vapor pressure. The glassware was cleaned in a freshly prepared sulfochromic solution, abundantly rinsed with triply distilled water, and dried before use. Surfactant solutions were prepared in the usual buffer previously purified by foaming. The surface of the surfactant solution was cleaned by aspiration just before each measurement. The surface tension was then monitored continuously as a function of time, using the Wilhelmy plate method. The recordings were stopped after the surface tension had reached a constant value.

Quasielastic light scattering

The quasielastic light scattering (QELS) measurements were performed with a nanosizer apparatus (Coulter Electronics). The scattered light was detected at 90°, and the samples were diluted with buffer to a 1 mM total lipid concentration just before measurement. In such high dilution conditions, the Stokes law can be applied, and the particle hydrodynamic radius (R_H) is given by the Stokes-Einstein equation (Candau, 1986):

$$D = k_B T/6\pi\eta R_H$$

where D is the free-particle diffusion coefficient, k_B is Boltzmann's constant, T is the absolute temperature, and η is the viscosity of the continuous phase. To take into account the sample size polydispersity, a unimodal analysis assuming a log-Gaussian distribution was used. For all samples, the standard deviation of three independent measurements was typically found to be lower than 5% of the R_H value.

High performance gel exclusion chromatography

Aggregate size distributions were determined using a HPLC apparatus already described (Ollivon et al., 1986; Lesieur et al., 1993). The 0.75 ×

30 cm TSK-G6000 PW column was supplied by Toyo Soda (Tokyo, Japan). The eluant (flow rate 1 ml/min) was the buffer used for vesicle preparations. Before each analysis series, the column was saturated with lipids. Sample loadings were 50 μl. Material detection was performed by on-line turbidity measurements with a Hitachi multichannel detector (model L-3000) in the 200–360 nm range. Elution volumes V_e were taken at the intercept of the half-height tangents of the elution peaks. Particle hydrodynamic diameters were deduced from the column parameter:

$$k_d = (V_e - V_o)/(V_t - V_o) \quad (1)$$

where V_o is the effective void volume (3.98 ml from elution of 1 μm phospholipidic vesicles), and V_t is the total volume (11.01 ml from elution of sodium azide) of the column, and according to the equation of the gel selectivity curve (Lesieur et al., 1993),

$$\log(MD) = 3.03 - 4.43k_d + 9.63k_d^2 - 8.85k_d^3 \quad (2)$$

Three independent sample injections provide mean diameter determinations with standard deviations from 5% to 10%, depending on the size range of the particles (Lesieur et al., 1993).

Cryogenic transmission electron microscopy

The technique used for the cryogenic transmission electron microscopy (cryo-TEM) examination has been described in detail elsewhere (Bellare et al., 1988; Dubochet et al., 1988), but consisted, in short, of the following. Thin, 10–500-nm sample films were prepared under controlled temperature (25°C) and humidity conditions within a custom-built environmental chamber. The films were thereafter vitrified by quick freezing in liquid ethane and transferred to a Zeiss EM 902 transmission electron microscope for examination. To prevent sample perturbation and the formation of ice crystals, the specimens were kept cool, below 108 K, during both the transfer and viewing procedures. All observations were made in zero-loss bright-field mode and at an accelerating voltage of 80 kV. To ensure reproducibility, the selection of micrographs presented in the article was chosen from a large number of negatives. For the evaluation of the cryo-TEM micrographs, it is important to realize that the two-dimensional projection of a closed liposome will appear as a circular object with enhanced contrast around the rim. This is due to the fact that the projected thickness of the bilayer shell is maximum at the edges. On the other hand, the projection of a flat bilayer disk will appear even in contrast right up to the edge.

Small-angle x-ray scattering

The preliminary x-ray scattering experiments were carried out on the D22 line of the DCI Synchrotron source at LURE (Orsay, France). The recordings were performed by using a radiation of wavelength 1.38 Å and a 1024 channel Xe-ethane-filled linear detector. The patterns were normalized with respect to Synchrotron beam decay, acquisition time, and punctually to sample transmission. The samples were prepared in a manner similar to that of the highly diluted mixtures, as described above, however without ultrasonic irradiation. Phase separation was performed in a narrow tube 5 mm in diameter, closed under argon. Thin glass capillaries (GLAS, Müller, Berlin) were used as sample cells for small-angle x-ray scattering (SAXS) measurements.

RESULTS

Surface properties of M-PEG-Chol compounds

Lowering of the surface tension of buffer by the addition of the cholesterol derivatives was observed whatever the chain length of the poly(ethylene glycol) moiety, showing that they are surface-active agents. The equilibrium surface tension versus surfactant concentration plots are reported in Fig. 3. The critical micelle concentrations (cmc) were determined from the breaks in the curves, which yielded 0.8 μM for M-PEG1000-Chol and 0.4 μM for M-PEG2000-Chol. Cryo-TEM analysis of polymer solutions at concentrations above the cmc confirms the existence of micelles. Whatever the molecular weight of the cholesterol derivative, they present a globular structure very close to that shown in Fig. 4 for M-PEG2000-Chol. The micellar diameters revealed for both compounds are close to the limit of the size resolution (1 nm) and contrast with the hydrodynamic diameters deduced from QELS measurements by assimilating the micelles to spheres (13 $\pm$ 3 nm and 12 $\pm$ 2 nm from M-PEG1000-Chol and M-PEG2000-Chol, respectively). This difference may be partly explained by the presence of a water layer at the micelle surface, contributing to the overestimation of their size by QELS. However, the 10-nm shift between the two diameter determinations strongly suggests that the electron density of the PEG chains is matched by buffer, so that they cannot be visualized by electron microscopy.

Cryo-TEM

Structural features of the $C_{16}G_2$/cholesterol/M-PEG-Chol mixed aggregates were revealed by cryo-TEM. All of the specimens were prepared within 2 weeks after ultrasonic irradiation. Samples containing M-PEG1000-Chol at molar ratios ranging from 2% to 30% were examined (Fig. 5). The incorporation of low polymer amounts ($\leq$5 mol%) gives rise to unilamellar and rather polydisperse vesicles, as shown in Fig. 5, *a* and *b*. Spherical vesicles with diameters mainly ranging from 20 nm to 200 nm coexist with elongated ones, comparable to cylinders and varying from 100 nm to more than 500 nm in length and from 40 nm to 80 nm in width. Increasing polymer content up to 10 mol% leads to a narrower size distribution. The elongated structures have almost disappeared, and vesicles, predominantly spheroidal, with diameters in the 35–170-nm range are formed (Fig. 5 *c*). At this stage, the particle membrane exhibits an irregular

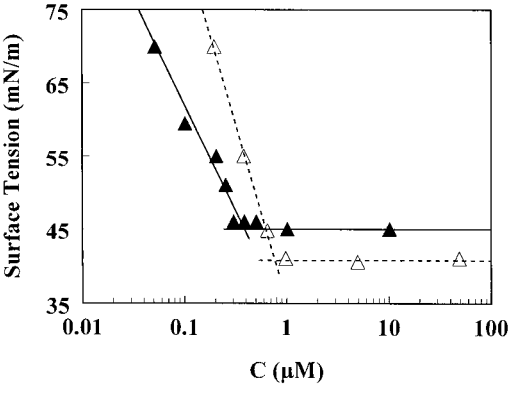

FIGURE 3 Surface tension-log concentration curves of M-PEG1000-Chol (△) and M-PEG2000-Chol (▲) in buffer.

FIGURE 4 Cryo-TEM picture of a 2 mM M-PEG2000-Chol micellar solution in buffer. Bar, 100 nm.

surface, as if the vesicles were delimited by a rippling bilayer. The sample containing 20% M-PEG1000-Chol shows two coexisting aggregate populations (Fig. 5 *d*). On one hand, vesicles are still present. They are mainly spherical and monodisperse, with 80–100-nm diameters. Some of the vesicles appear to have openings. On the other hand, disk-shaped aggregates, very likely bilayer fragments, can be observed either edge on, face on, or at all orientations in between. The disks are nearly 4 nm thick and vary from 15 nm to 130 nm in diameter. Finally, at 30 mol%

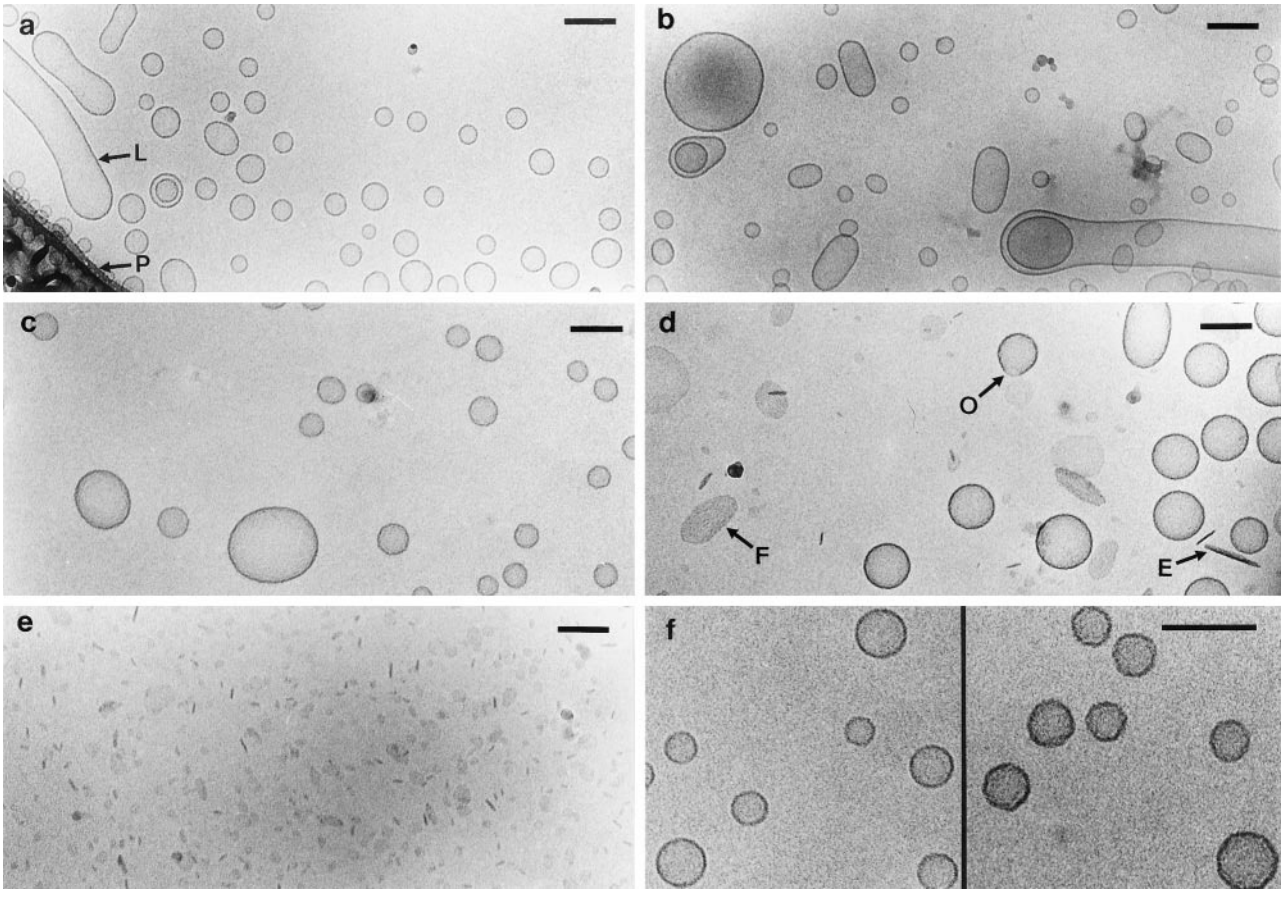

FIGURE 5 Cryo-TEM pictures of $C_{16}G_2$/cholesterol/M-PEG1000-Chol (50/50-*x*/*x* mol%) mixed aggregates. The total lipid concentration is 2 mM. (*a*) $x = 2$ mol%: a majority of small unilamellar vesicles can be seen with either spherical or elongated shapes. Some long cylindrical structures (L) are also observed; the polymer film (P) is included in the picture for clarity. (*b*) $x = 5$ mol%: structures similar to the preceding ones. (*c*) $x = 10$ mol%: spheroidal unilamellar vesicles showing an irregular bilayer surface. (*d*) $x = 20$ mol%: unilamellar vesicles, almost all of them spherical, coexist with discoid aggregates seen either edge on (E) or face on (F) or at all orientations in between. Some of the vesicles appear open (O). (*e*) $x = 30$ mol%: the mixed aggregates are viewed as bilayered disks. (*f*) Vesicles belonging to samples containing $x = 2$ mol% (*left side of the picture*) and $x = 10$ mol% (*right side of the picture*) M-PEG1000-Chol. The enrichment in polymer clearly generates rough vesicles. Bar, 100 nm.

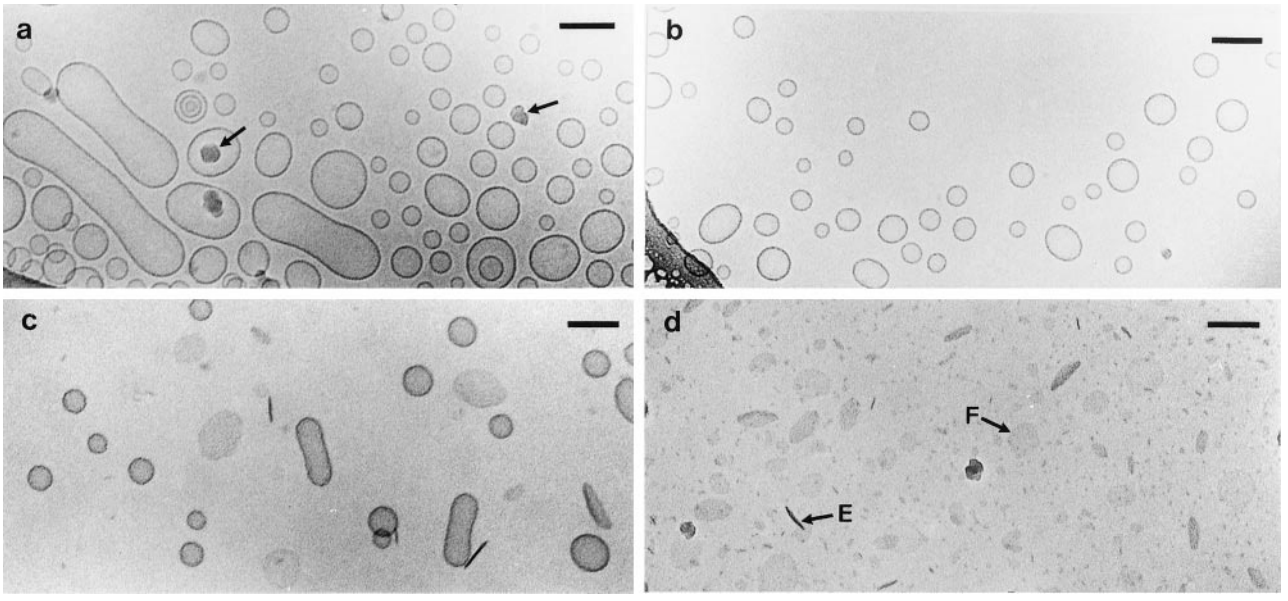

FIGURE 6 Cryo-TEM pictures of $C_{16}G_2$/cholesterol/M-PEG2000-Chol (50/50-*x*/*x* mol%) mixed aggregates. The total lipid concentration is 2 mM. (*a*) $x = 2$ mol%: spherical and elongated vesicles, mostly unilamellar, coexist. Arrows denote some frost deposited on the sample after vitrification. (*b*) $x = 5$ mol%: single-walled spheroidal vesicles with apparently wavy external surface can be seen. (*c*) $x = 10$ mol%: mostly spherical unilamellar vesicles are revealed beside sparse peanut-shaped ones, in coexistence with disk-shaped aggregates. (*d*) $x = 20$ mol%: only discoid structures are observed edge on (E) or face on (F). Bar, 100 nm.

M-PEG1000-Chol, no more vesicles, but only disk-shaped aggregates are observed (Fig. 5 *e*). Their diameter is reduced compared to the preceding sample and does not exceed 30 nm.

Samples containing M-PEG2000-Chol present a very similar behavior (Fig. 6). Nevertheless, the characteristic steps of the aggregate evolution correspond to polymer ratios systematically lower than those noticed for the M-PEG1000-Chol-based system. At 2 mol% M-PEG2000-Chol, only vesicles, mainly unilamellar, are observed (Fig. 6 *a*). Spherical structures (diameters from 25 nm to 100 nm) coexist with elongated or peanut-shaped arrangements (width ~80 nm, length several hundred nanometers). With an increasing polymer level of 2–5 mol% (Fig. 6 *b*), the particle shape polydispersity decreases significantly, to the detriment of elongated structures, and the vesicles begin to present an undulating surface. Incorporation of 10 mol% M-PEG2000-Chol induces the appearance of disk-shaped aggregates in addition to the remaining undamaged vesicles (Fig. 6 *c*). The pictures corresponding to higher polymer ratios reveal the formation of only disk-like structures, with diameters ranging from several to a hundred nanometers (Fig. 6 *d*).

QELS analysis

The apparent diffusion coefficients *D* of the $C_{16}G_2$/cholesterol/M-PEG-Chol (50/50-*x*/*x* mol%) mixed aggregates were measured at a 90° scattering angle. For each sample, nearly constant values were recorded over a 2-week period (Fig. 7), indicating appreciable size stability of the aggregates whatever the polymer molar ratio and chain length. Table 1 shows the evolution with time of the mean hydrodynamic diameter ($2R_H$) for the aggregates containing either 10 mol% M-PEG1000-Chol or 5 mol% M-PEG2000-Chol, which are indeed seen to be mostly spherical in the cryo-TEM pictures. The very slight fluctuations in the size parameters, including $2R_H$ and standard deviation values, illustrate the aggregate stability. This last is very comparable to that observed for nonionic surfactant vesicles (NSVs)

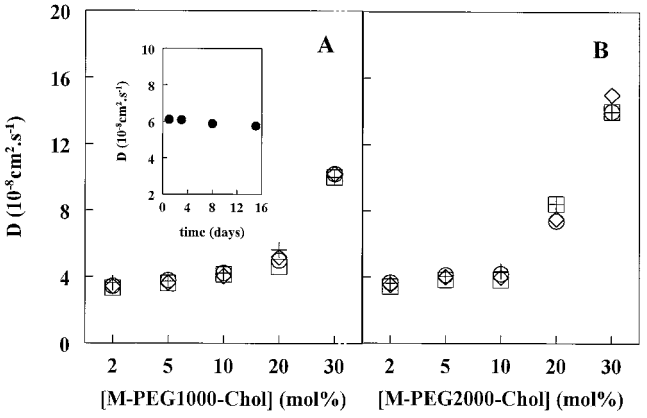

FIGURE 7 Evolution of the apparent diffusion coefficient of the (*A*) $C_{16}G_2$/cholesterol/M-PEG1000-Chol (50/50-*x*/*x* mol%) and (*B*) $C_{16}G_2$/cholesterol/M-PEG2000-Chol (50/50-*x*/*x* mol%) mixed aggregates as a function of polymer ratio, after storage periods of 1 (+), 3 (◇), 8 (○), and 15 (□) days. The inset shows the variation in the apparent diffusion coefficient with time for NSV ($C_{16}G_2$/cholesterol/DCP: 48.0/48.4/3.6 mol%). The QELS analyses were performed at a 90° scattering angle.

TABLE 1 Mean hydrodynamic diameters ($2R_H$) over a 15-day period after preparation of the spheroidal $C_{16}G_2$/cholesterol/M-PEG-Chol vesicles

	M-PEG1000-Chol x = 10 mol%*		M-PEG2000-Chol x = 5 mol%*	
Time (days)	$2R_H$ (nm)	SD# (nm)	$2R_H$ (nm)	SD# (nm)
	99	36	103	36
3	100	38	102	35
8	97	36	100	33
15	104	33	112	38

*x is the polymer molar ratio of the mixed aggregates composed of $C_{16}G_2$/cholesterol/M-PEG-Chol (50/50-x/x mol%)
#The standard deviation corresponds to a unimodal analysis assuming a log-Gaussian particle size distribution.

composed of $C_{16}G_2$ and cholesterol and stabilized by a low proportion of the negatively charged compound DCP (Fig. 7, *inset*, and Seras et al., 1992).

The comparison of the QELS diameters shown in Table 1 with sizes reported by cryo-TEM (Figs. 5 *c* and 6 *b*) deserves attention. A tendency of QELS to overestimate the effective geometrical diameter of the particles can be noticed, especially in the case of the M-PEG2000-Chol aggregates. Given the nonnegligible standard deviations measured, this is due partly to the weighting toward the larger particles in a polydisperse system, inherent in QELS measurements, as has been both experimentally and theoretically demonstrated (Wong and Thompson, 1982). The possibility is also not excluded that, because of the presence of hydrophilic PEG chains at their surface, the vesicles drag water molecules in their Brownian motion, so that their hydrodynamic radius appears larger than the geometric one (Corti, 1985). In the latter hypothesis and according to our results, the hydration effect would be more important for PEG chains with a molecular weight of 2000.

HPLC-GEC analysis

Sizing of M-PEG-coated aggregates was also performed by high-performance gel exclusion chromatography (HPLC-GEC) coupled with turbidity on-line detection. The analysis was carried out 1 week after sample preparation. Fig. 8,*a* and *b*, shows the chromatograms obtained as a function of polymer chain length and molar ratio. NSVs were also analyzed as a reference. Most of the gel exclusion patterns present similar shapes consisting of nearly symmetrical peaks, attributable to unimodal size distributions. Some of the elution profiles also display a very slight shoulder (V_e = 10.81 ml) close to the total volume of the column and thus corresponding to very small particles. This shoulder tends to be amplified by high M-PEG-Chol contents. For low polymer ratios as well as for NSVs, the maxima of the chromatograms, i.e., the hydrodynamic sizes, are varying in a very narrow interval (V_e, from 8.42 to 8.55 ml). At intermediate polymer levels corresponding to the vesicle-disk coexistence domain revealed by cryo-TEM, the GEC profiles only account for unimodal size distributions due to size closeness between both types of aggregates. In return, aggregates containing 30 mol% of M-PEG1000-Chol or from 20 mol% to 30 mol% of M-PEG2000-Chol display significant shifts of their GEC peaks toward the elution region of smaller particles (V_e, from 9.05 to 9.67 ml), compared to vesicle elution range. This progressive decrease in size with increasing polymer molecular weight or molar ratio depicted by HPLC-GEC agrees with the size decrease observed in the disk domain by cryo-TEM.

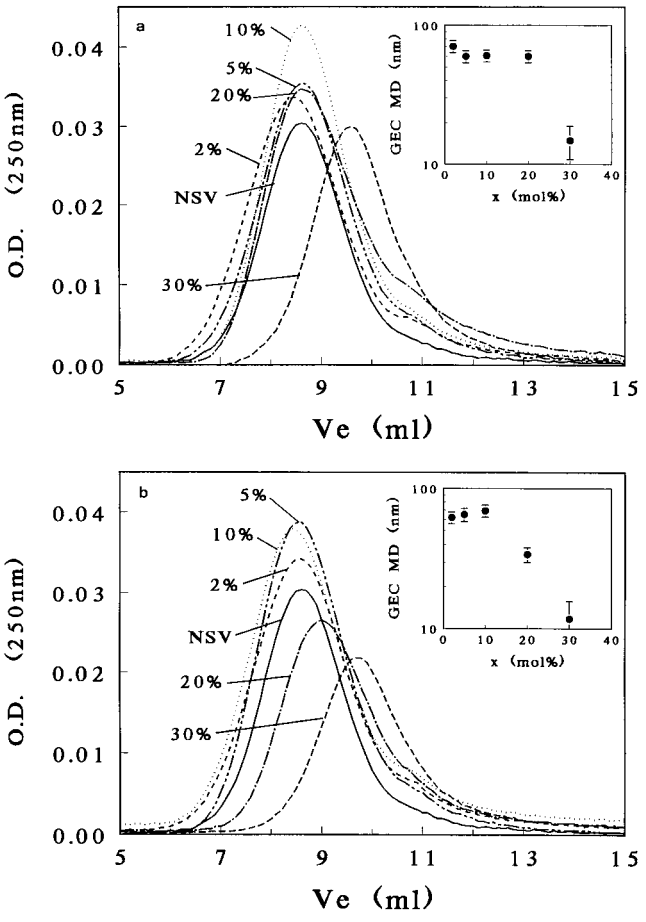

FIGURE 8 HPLC gel exclusion profiles of NSV ($C_{16}G_2$/cholesterol/DCP: 48.0/48.4/3.6 mol%) and $C_{16}G_2$/cholesterol/M-PEG-Chol (50/50-x/x mol%) mixed aggregates 1 week after ultrasonic irradiation, relative to M-PEG1000-Chol (*a*) and M-PEG2000-Chol (*b*). Percentages refer to M-PEG-Chol molar ratios x and V_e to the elution volume. HPLC patterns were performed with 50-μl sample loading and a eluant flow rate of 1 ml/min. The effective void volume of the column was 3.98 ml (from elution of 1 μm phospholipidic vesicles), and the total volume was 11.01 ml (from elution of sodium azide). The insets show the evolution versus M-PEG-Chol content of the mean hydrodynamic diameter, deduced from the k_d value at the maximum of the chromatograms and Eq. 2 (see Materials and Methods).

Mean hydrodynamic diameters were calculated from the TSK G6000 PW selectivity curve already established (Lesieur et al., 1993), and are reported in the insets of Fig. 7, *a* and *b*. The results are in accord with the size distributions observed by cryo-TEM, when limited to spheroid or discoid

particles. In return, the GEC MD found at M-PEG1000-Chol and M-PEG2000-Chol ratios lower than 10 mol% and 5 mol%, respectively, and the unimodal elution profiles do not reveal the length of the large rod-like aggregates that should be eluted at the void volume of the column. This suggests that, under the HPLC conditions that impose a flow constraint, the cylindrical vesicles may be allowed to penetrate lengthwise the pores of the gel, so that the retention times only report the cylinder widths (Seras et al., 1996). Indeed, HPLC-GEC indicates MD values in the 60–70-nm range, which coincides with the range of cylinder widths seen in micrographs.

DISCUSSION

Characteristics of the M-PEG-Chol conjugates

The formation of a stable lamellar phase by mixing lipids and a PEG-lipid conjugate depends not only on the nature of the hydrophobic residue of the conjugate, but also on its hydrophilic chain length (Torchilin, 1996; Allen, 1994a; Bedu-Addo and Huang, 1995; Hristova et al., 1995; Kenworthy et al., 1995b). The adjustment of the latter results from the compromise between optimizing the steric barrier by using rather long PEG chains and minimizing mixed micelle formation. The hydrophilic-lipophilic balance should also be chosen to lower the water solubility of the PEGylated surfactant. That is, values of cmc that are too high strongly limit incorporation levels of the surfactant in lipid bilayers and dramatically favor its removal from the vesicles upon dilution. According to studies on PEGylated phospholipids, the best miscibilities with guest phospholipidic lamellar phases were typically obtained for PEG molecular weights of 1000–5000 (Bedu-Addo and Huang, 1995; Bedu-Addo et al., 1996a,b). The same result was recently described in the case of PEG cholesteryl ether (Ishiwata et al., 1995; Vertut-Doï et al., 1996). In the biological environment, the protection against phagocytosis was improved with increasing PEG chain length up to a molecular weight of 2000, whereas beyond this value, blood circulation times are not significantly changed (Allen et al., 1991). These reports incited us to restrict our study to the examination of the two PEG molecular weights, a priori delimiting the most efficient chain lengths, i.e., 1000 and 2000, respectively. The corresponding M-PEG cholesteryl carbonates advantageously display very low solubilities in buffer with cmc plainly below 1 μM, against 6 μM reported in saline medium conditions for PEG1900-DSPE (Uster et al., 1996) and 2–4 μM for PEG2200 cholesteryl ether (Ishiwata et al., 1995) in water. However, in the latter case, the difference may arise from the presence of 145 mM NaCl in our buffer, which may reduce the surfactant solubility, as already suggested in the case of phospholipidic derivatives (Lasic, 1994). Unlike what is generally observed for alkyl ethylene oxide (EO) surfactants containing less than 10 EO units (Becher, 1966), M-PEG-Chol exhibit decreasing cmc with increasing PEG chain length, even when cmc is expressed in units of weight per volume (1.13 mg/liter for M-PEG1000-Chol and 0.72 mg/l for M-PEG2000-Chol). This has also been observed in the case of the cholesteryl ether derivatives with PEG molecular weights ranging from 2200 to 8800 (Ishiwata et al., 1995). Such a behavior seems more plausibly inherent in the cholesterol hydrophobic moiety rather than in water solubility differences of PEG chains, especially in the 20–45-EO unit range.

Aggregation behavior of highly hydrated $C_{16}G_2$/cholesterol/M-PEG-Chol mixtures

The images revealed in this study outline three main structural domains as a function of polymer level. Below 10 mol% M-PEG1000-Chol or 5 mol% M-PEG2000-Chol, only vesicles are formed: the absence of micelles on the cryo-TEM pictures and GEC profiles shows the highly efficient incorporation of PEGylated cholesterol into the $C_{16}G_2$/cholesterol assemblies, while preserving closed bilayered structures, stable over 2 weeks at least. Polymer saturation ratios of 20 mol% M-PEG1000-Chol or 10 mol% M-PEG2000-Chol yield two coexisting particle populations: vesicles and disk-shaped bilayer fragments. Finally, higher M-PEG-Chol amounts lead to the disappearance of the vesicles; only disks are obtained.

The vesicular domain shows sensitivity of both geometry and size of the particles to the M-PEG-Chol membrane composition. Very low polymer levels produce heterogeneous vesicle populations composed of coexisting spherical and cylindrical units. An increase in M-PEG-Chol content reduces the shape polydispersity by favoring the formation of spherical vesicles. The best homogenization of the populations is reached at the saturation of the lipids bilayers in polymer, i.e., when the disks begin to form. The ability of PEGylated compounds to transform deformed vesicles into nearly calibrated and spherical ones has also been depicted for systems based on PEGylated phosphatidylethanolamine (PEG-PE) and phospholipids associated (Edwards et al., 1996) or not (Lasic et al., 1991) with cholesterol. Such morphological evolution is comparable to that already observed when the solubilizing surfactant octyl glucoside (OG) was added to NSVs (Seras et al., 1996) or to egg phosphatidylcholine vesicles (Vinson et al., 1989). Shape and size transformations of the mixed vesicles were interpreted as a function of the distribution of the surfactant molecules among the lipidic assemblies. For the NSV-OG system, time-resolved fluorescence experiments demonstrated that the appearance of elongated structures at low surfactant compositions corresponds to the heterogeneous location of OG within the vesicle membrane, whereas spherical particles observed at high surfactant content present uniform molecular distribution (Seras et al., 1992, 1994, 1996). It can be expected that the bilayer curvature of the $C_{16}G_2$/cholesterol/M-PEG-Chol mixed vesicles is similarly governed by the distribution of the polymer derivative in the lipidic matrix.

In the vesicle-disk coexistence domain, open vesicles are seen in the micrographs. This observation is not new, because open vesicles have been visualized by cryo-TEM in a number of other lipid-surfactant systems (Walter, 1992). The images presented in this study show properly vitrified films, giving evidence that the quenching of the samples by freezing in CEVS conditions was almost instantaneous (Dubochet et al., 1988), which should not allow comparably slow major rearrangements of the lipid molecules to produce an open vesicle. It is more probable that these rearrangements occur in the samples before specimen preparation and are only connected with the polymer enrichment, because no open vesicles are revealed at subsaturation levels of M-PEG-Chol. Nevertheless, even if the opening of the vesicles was, in a certain extent, due to the sample filming procedure, this would be evidence of vesicle brittleness at high polymer incorporation. Accordingly, it has been demonstrated that grafting polymers to lipid bilayers affects the area compressibility modulus of the bilayers and hence reduces their mechanical stability (Hristova and Needham, 1994).

The third domain described by the cryo-TEM pictures is only constituted of disks and appears to be optically isotropic. The aggregate thickness, estimated to be 4 nm, is equal to the hydrophobic thickness of a dehydrated $C_{16}G_2$/cholesterol (50/50 mol%) bilayer (Vanlerberghe et al., 1978). By considering that the PEG chains are not revealed by this technique (see the Results), it implies that the disk core is composed of flat sheets of uninterdigitated lipid bilayer. Similarly, it has been already shown by x-ray diffraction that the incorporation of high levels of PEG2000-DSPE into distearoylphosphatidylcholine bilayers does not induce lipid interdigitation (Kenworthy et al., 1995b). The formation of bilayered disks has also been observed for phospholipid/cholesterol/PEG-PE mixtures: the perfectly planar and circular forms, as well as the preservation of disk shape, at high PEGylated lipid levels instead of transformation into thread-like micelles, have been shown to be specific for cholesterol-containing aggregates (Edwards et al., 1996). Despite the nonnegligible polydispersity of the disk populations, both cryo-TEM and HPLC-GEC clearly show the decrease in disk diameter with increasing polymer proportion. This suggests the preferential location of the polymer at the disk circumference: the disk core would be based on a $C_{16}G_2$/cholesterol/M-PEG-Chol mixed bilayer saturated in polymer, whereas the exceeding M-PEG-Chol molecules would constitute the edges of the disks. This model has already been proposed for bile salt-phospholipid mixtures (Mazer et al., 1990).

Conformation of the PEG chains at the vesicle surface

The structural state of the polyoxyethylenic chains coating the vesicles can be predicted by the scaling laws describing the conformation of flexible polymer chains grafted to a planar surface and immersed in a good solvent (Alexander, 1977; de Gennes, 1980). Indeed, PEG is highly soluble in the aqueous buffer used in this study. In addition, the vesicle shell can be reasonably approximated to a planar surface, assuming the particle diameters to be very large compared to the maximum PEG chain extension, expected to be below 6 nm from both experimental data (Kuhl et al., 1994; Kenworthy et al., 1995b) and theoretical calculation (see Table 2). By comparing the average distance between grafting sites, d, to the Flory radius, $R_F = N^{3/5}a$, given for a coiled chain in a good solvent with N monomer units of length a, two principal regimes have been defined (de Gennes, 1980): for $d > R_F$, the polymer develops as separate coils or mushrooms, whereas for $d < R_F$, the chains overlap and adopt a stretched state or brush regime. In this second case, the thickness of the grafted polymer layer is $L \cong Na^{5/3}/d^{2/3}$. The d values as well as the nature of the PEG chain conformation and their extension L in the brush regime are reported in Table 2. It is worth noting that our calculated L values for the extended length of M-PEG2000 chains agree well with values ranging from 35 Å to 50–65 Å, experimentally determined from other lipidic systems, by increasing the PEG2000-lipid molar ratio from 5 mol% to 10 mol% (Janzen et al., 1996; Hristova et al., 1995; Kuhl et al., 1994; Kenworthy et al., 1995a,b; Shimada et al., 1995; Woodle et al., 1992). This agreement reasonably validates the theoretical calculations of the PEG coating thicknesses in our study.

The conformation transition from mushrooms to brushes, at a molar ratio x close to 7.5 mol% M-PEG1000-Chol or 3.5 mol% M-PEG2000-Chol, interestingly coincides with the disappearance of the elongated vesicle shapes accompanied by size decrease and bilayer curvature homogenization. It is conceivable that the important steric repulsions

TABLE 2 Theoretical distance between grafting sites, *d*, and brush thickness, *L*, of the PEG chains, as a function of their length and grafting density at the vesicle surface.

		M-PEG1000-Chol		M-PEG2000-Chol	
x (mol%)*	d (Å)#	Conformation§	L (Å)¶	Conformation§	L (Å)¶
2	44	M	—	M	—
5	28	M	—	B	39
10	18	B	27	B	53
20	14	B	32	—	—

*Vesicles composed of $C_{16}G_2$/cholesterol/M-PEG-Chol (50/50-x/x mol%)

#The distance between grafting sites d was calculated from the polymer molar fraction x and the average surface area given for a $C_{16}G_2$/cholesterol (50/50 mol%) bilayer (Vanlerberghe et al., 1978), according to the expression $d = (39/x)^{1/2}$ (Kenworthy et al., 1995).

§The conformation state of the PEG chains at the vesicle surface was derived from the comparison of the distance d between grafting sites and the Flory radius, $R_F = N^{3/5}a$, of the M-PEG polymers. R_F values calculated for M-PEG1000 ($N = 23$) and M-PEG2000 ($N = 45$) moieties are 23 Å and 34 Å, respectively, taking $a = 3.5$ Å (Kuhl et al., 1994; Kenworthy et al., 1995a, b). N, OE unit number; a, OE unit length. Mushroom (M) or brush (B) regimes correspond to $d < R_F$ or $d > R_F$.

¶The extended length of the PEG chains in the brush regime is given by $L \cong Na^{5/3}/d^{2/3}$ (de Gennes, 1980).

between the M-PEG-Chol headgroups caused by their denser distribution impose a random distribution of the polymer to minimize chain overlapping, which is in favor of a spherical shape. The denser distribution of the brush may generate packing irregularities of the lipid molecules, as suggested by the rough vesicle surface seen in the micrographs (Figs. 5 *c*, *f* and 6 *c*). On the other hand, the QELS measurements demonstrate the size stability with time of the M-PEG-Chol-coated vesicles, proving the efficiency of M-PEG-Chol in creating a steric barrier at the particle surface, preventing them from self-aggregation and fusion. Regarding biological applications, the achievement of stable vesicles coated by PEG chains in the brush conformational state is encouraging; previous investigations have actually demonstrated that liposome stealthiness is improved by increasing both PEG chain extension and density (Lasic, 1996; Needham et al., 1992).

However, there is a limit to the density of the PEG chains in the brush regime: a too high polymer content leads to vesicle disruption and disk formation. The impossibility, at this stage, of bending the bilayer may arise from an increase in the lateral steric repulsion between neighboring chains. At the M-PEG-Chol saturation levels (between 10 mol% and 20 mol% M-PEG1000-Chol or 5 mol% and 10 mol% M-PEG2000-Chol), the theoretical model forecasts PEG thicknesses close to 30 Å or 45 Å, against 23 Å and 34 Å in the mushroom regime, depending on the PEG molecular weight (Table 2). Given that the volume occupied by one hydrophilic chain remains unchanged, the stretching of the chains necessarily leads to the modification of the geometrical balance between polar headgroups and cholesterol anchors that would be in favor of a minimum curvature. The consequence, unsuited to drug carrier applications, is the generation of open structures, leading to the loss of encapsulated material.

Vesicle to disk transition

Transition from vesicles to open structures with increasing PEGylated lipid content and involving an intermediate domain in which both types of particles coexist, has been already described for phospholipids/cholesterol/PEG-PE systems and interpreted in terms of vesicle-to-micelle transition (Lasic et al., 1991; Edwards et al., 1996). Concurrently, structural investigations undertaken on these systems or analogs have demonstrated the lamellar to micellar phase conversion triggered by increasing the PEG derivative composition (Kenworthy et al., 1995b; Hristova et al., 1995; Bedu-Addo and Huang, 1995b; Bedu-Addo et al., 1996a,b). The solubilization of NSVs upon the addition of PEG cholesteryl conjugates has been reported as well (Uchegbu et al., 1992; Chopineau et al., 1994), and confirmed by the corresponding partial phase diagram (Uchegbu et al., 1996). As inspired from these reports, the rupture of the vesicles into disk-shaped assemblies should correspond to the onset of the lipid solubilization by the M-PEG-Chol derivatives, insofar as these last are surface-active agents. That is, the first dissolution step of the $C_{16}G_2$/cholesterol lamellar assemblies may be their separation into individual bilayered particles stabilized by the surfactant molecules.

The boundary between vesicle and vesicle-disk coexistence domains corresponds to a polymer saturation level of the lipidic membrane in the 10–20 mol% M-PEG1000-Chol and 5–10 mol% M-PEG2000-Chol ranges, respectively. Similar critical ratios have been found when PEG-PE derivatives (Lasic et al., 1991; Allen et al., 1991; Schneider et al., 1996; Hristova et al., 1995; Edwards et al., 1996), as well as PEG cholesteryl ether (Ishiwata et al., 1995; Vertut-Doï et al., 1996) or hemisuccinate (Schneider et al., 1996), are incorporated into liposomes. A decrease in the saturation level of the lipid lamellar assemblies with increasing PEG molecular weight has also been observed (Allen et al., 1991; Ishiwata et al., 1995; Kenworthy et al., 1995b) and attributed to the increase in bulkiness of the polymer polar headgroup with the PEG chain lengthening (Hristova and Needham, 1994). Complete vesicle disappearance, i.e., the beginning of the pure disk domain, also requires more M-PEG1000-Chol (in the 20–30 mol% range) than M-PEG2000-Chol (in the 10–20 mol% range); the longer the PEG chain, the better the destabilizing ability. By assuming the concentration of M-PEG-Chol in buffer to be negligible, because they should not exceed 1 μM with regard to the cmc values of the pure PEGylated compounds, the surfactant-to-lipid molar ratios in the aggregates can be directly calculated from the total concentrations of both constituents. Thus, at the onset of the disk domain, these ratios can be estimated to ~0.4 or ~0.2 for M-PEG1000-Chol or M-PEG2000-Chol, respectively. During NSV solubilization by the PEG cholesteryl ether derivative Solulan C24 (Uchegbu et al., 1992), the formation of turbid intermediate structures replacing initial vesicles has been found at a close surfactant-to-lipid molar ratio of 0.3, These intermediates, unfortunately undefined in the reported study, may correspond to disk-like aggregates similar to those seen in our study.

Although further work is certainly required to definitively assimilate the disks into a micellar phase, there are already several points in favor of this hypothesis. One argument is the delimitation of the coexistence domain, in the M-PEG-Chol-rich region, by only disked-shaped structures with stable, finite, and rather small dimensions, decreasing in size with increasing polymer level. We also observed that less diluted preparations (85% hydration by weight), located in the intermediate polymer concentration domain, separate with time into a dense and turbid phase and a clear supernatant phase. Preliminary SAXS investigations provided information on the structural arrangement of each phase. The small-angle SAXS pattern of the upper phase (Fig. 9 *b*) is characterized by two rather broad diffraction peaks contrasting in intensity and centered at 0.025 $Å^{-1}$ and 0.070 $Å^{-1}$, respectively. The location of these peaks does not reflect a lamellar organization. Moreover, this pattern appears very close in shape to that recorded from pure M-

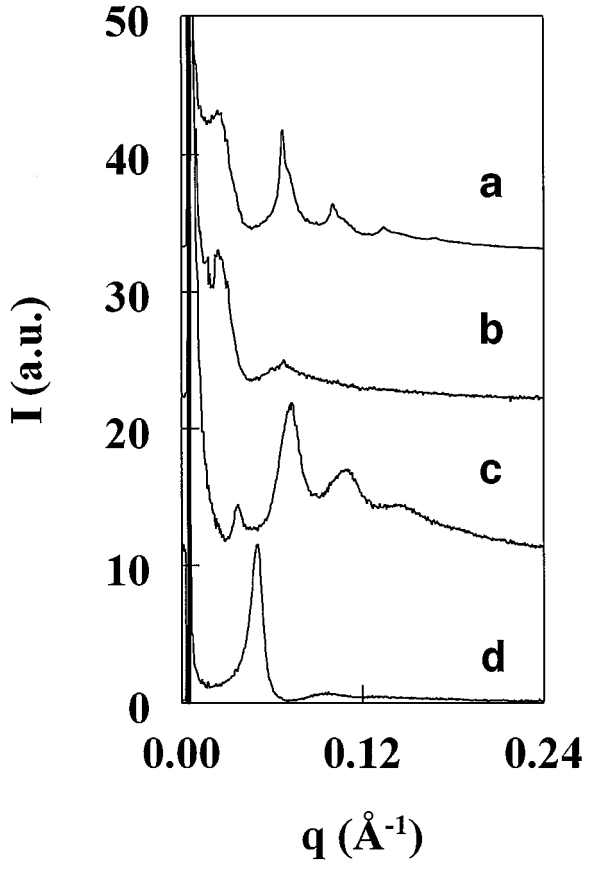

FIGURE 9 Small-angle x-ray diffraction patterns of hydrated (85% of buffer by weight) $C_{16}G_2$/cholesterol/M-PEG2000-Chol mixtures. (*a*) Coexistence domain (15 mol% M-PEG2000-Chol), total sample. (*b*) Coexistence domain (15 mol% M-PEG2000-Chol), upper phase. (*d*) Pure lamellar domain (5 mol% M-PEG2000-Chol). Pattern *c* corresponds to a 55.8 mM M-PEG2000-Chol solution in buffer (86.5 wt% hydration).

PEG-Chol concentrated micelles (Fig. 9 *d*), except for the relative shift of the two patterns. This result supports the possibility that the structure of the upper phase formed in the coexistence domain is governed by the polymer-based surfactant and probably corresponds to a micelle-like arrangement. As a tentative interpretation, by attributing the very intense peak seen at lower angles to a structure factor contribution, this phase may be composed of the disks seen by cryo-TEM, however, in strong interactions due to the low hydration of the sample examined by SAXS. The whole sample (Fig. 9 *a*), before macroscopic phase separation, exhibits the superimposition of the peaks characteristic of the upper phase, with four sharp Bragg reflections at 0.068 $Å^{-1}$, 0.101 $Å^{-1}$, 0.135 $Å^{-1}$, and 0.168 $Å^{-1}$, corresponding to the second to the fifth orders of a single lamellar structure of period 187 Å. Likely due to the contribution of the form factor of the lamellae (Nallet et al., 1993), the first-order peak that should be located at 0.033 $Å^{-1}$, has vanished. As complementary information, Fig. 9 *c* shows a diffraction pattern example of the lamellar phase formed before the coexistence domain and for which the first-order reflection is resolved.

The above observations underscore that the vesicular structures and the disks originate from two distinct phases. Consequently, the appearance of discoid assemblies corresponds to an effective phase transition phenomenon. Moreover, unlike the vesicles, the disks seen in the water-rich region of the phase diagram do not appear as the continuation of a lamellar phase, and seem, rather, to be related to a micellar phase.

CONCLUDING REMARKS

Among the main outlines resulting from this study, it has been shown that new sterically stabilized vesicles can be elaborated from the association of the synthetic nonionic monoalkyl lipid $C_{16}G_2$ and cholesterol, by grafting, via a carbonate bond, a PEG chain to a small part of the cholesterol molecules. The physical stability of these vesicles, over 14 days at least, added to the impermeability expected for the equimolar $C_{16}G_2$/cholesterol membrane, and constitutes a relevant asset with respect to potential drug delivery applications. However, the incorporation of the PEGylated cholesterol derivative shows two antagonistic effects, depending on its proportion. Whereas low levels do contribute to steric stabilization of the vesicles, high levels yield their inevitable destruction. The analogy between this phase behavior and a vesicle-to-micelle transition mechanism rather ranks M-PEG-Chol among the solubilizing amphiphiles. The membrane saturation threshold at which the closed bilayered aggregates are transformed into open disk-like structures depends on the polymer molecular weight and corresponds to the density of the PEG chains in their brush conformational state. Taking into account that the most homogeneous vesicle populations are formed at the beginning of the overlapping coils regime, it happens that the membrane composition in PEGylated lipid has to be chosen with the greatest care, to optimize the aggregate morphology, as well as the coating thickness responsible for the particle steric repulsion, while avoiding the formation of disks that would be detrimental to drug encapsulation. Such a compromise should correspond to ~10 mol% M-PEG1000-Chol or ~5 mol% M-PEG2000-Chol. On the basis of this physicochemical insight, further investigations concerning the vesicle's encapsulation efficiency as well as its resistance in the biological environment have been undertaken (Beugin-Deroo et al., 1998).

This work is part of S. Beugin's thesis, financially supported by the CNRS (bourse de docteur ingénieur). $C_{16}G_2$ and DCP were kindly provided by Dr A. Ribier (L'Oréal, France). The authors address special thanks to Drs. G. Mahuteau and D. Desmaële for helping with the RMN characterization of the M-PEG-Chol conjugates and M.-M. Boissonnade for advice concerning the surface tension measurements. The authors are particularly grateful to Dr. P. Lesieur for his helpful interventions in the x-ray diffraction analyses.

REFERENCES

Akiyoshi, K., and J. Sunamoto. 1992. Physicochemical characterization of cholesterol-bearing polysaccharides in solution. *In* Organized Solutions.

S. E. Friberg and B. Lindman, editors. Marcel Dekker, New York. 290–304.

Allen, T. M. 1992. Stealth liposomes: five years on. *J. Liposome Res.* 2:289–305.

Allen, T. M. 1994a. The use of glycolipids and hydrophilic polymers in avoiding rapid uptake of liposomes by the mononuclear phagocyte system. *Adv. Drug Del. Rev.* 13:285–309.

Allen, T. M. 1994b. Long-circulating (sterically stabilized) liposomes for targeted drug delivery. *Trends Pharmacol. Sci.* 15:215–220.

Allen, T. M. 1995. Long-circulating (stealth) liposomes, therapeutic applications. *In* Liposomes, New Systems and New Trends in Their Applications. F. Puisieux, P. Couvreur, J. Delattre, and J. P. Devissaguet, editors. Editions de Santé, Paris. 123–155.

Allen, T. M., C. Hansen, F. Martin, C. Redemann, and A. Yau-Young. 1991. Liposomes containing synthetic lipid derivatives of poly(ethylene glycol) show prolonged circulation half-lives in vivo. *Biochim. Biophys. Acta.* 1066:29–36.

Allen, T. M., and D. Papahadjopoulos. 1993. Sterically stabilized ("stealth") liposomes: pharmacokinetic and therapeutic advantages. *In* Liposome Technology. CRC Press, Boca Raton, FL. 59–72.

Alexander, S. 1977. Adsorption of chain molecules with a polar head. A scaling description. *J. Physiol. (Paris).* 38:983–987.

Azmin, M. N., A. T. Florence, R. M. Handjani-Vila, J. F. B. Stuart, G. Vanlerberghe, and J. S. Whittaker. 1985. The effect of non-ionic surfactant vesicle (niosome) entrapment on the absorption and distribution of methotrexate in mice. *J. Pharm. Pharmacol.* 37:237–242.

Azmin, M. N., A. T. Florence, R. M. Handjani-Vila, J. F. B. Stuart, G. Vanlerberghe, and J. S. Whittaker. 1986. The effect of niosomes and polysorbate 80 on the metabolism and excretion of methotrexate in the mouse. *J. Microencapsul.* 3:95–100.

Baillie, A. J., G. H. Coombs, T. F. Dolan, and J. Laurie. 1986. Non-ionic surfactant vesicles, niosomes, as a delivery system for the anti-leishmannial drug, sodium stibogluconate. *J. Pharm. Pharmacol.* 38: 502–505.

Becher, P. 1966. Micelle formation in aqueous and nonaqueous solutions. *In* Nonionic Surfactants. M. J. Schick, editor. Marcel Dekker, New York. 478–515.

Bedu-Addo, F. K., and L. Huang. 1995. Interaction of PEG-phospholipid conjugates with phospholipid: implications in liposomal drug delivery. *Adv. Drug Del. Rev.* 16:235–247.

Bedu-Addo, F. K., P. Tang, Y. Xu, and L. Huang. 1996a. Effects of polyethyleneglycol chain length and phospholipid acyl chain composition on the interaction of polyethyleneglycol-phospholipid conjugates with phospholipid: implication in liposomal drug delivery. *Pharm. Res.* 13:710–717.

Bedu-Addo, F. K., P. Tang, Y. Xu, and L. Huang. 1996b. Interaction of polyethyleneglycol-phospholipid conjugates with cholesterol-phosphatidylcholine mixtures: sterically stabilized liposome formulations. *Pharm. Res.* 13:718–724.

Bellare, J. R., H. T. Davis, L. E. Scriven, and Y. Talmon. 1988. Controlled environment vitrification system (CEVS): an improved sample preparation technique. *J. Electron. Microsc. Technol.* 10:87–111.

Beugin-Deroo, S., M. Ollivon, and S. Lesieur. 1998. Bilayer stability and impermeability of noniomic surfactant-vesicles sterically stabilized by PEG-cholesterol conjugates. *J. Colloid Interface Sci.* In press.

Blume, G., G. Cevc, M. D. J. A. Crommelin, I. A. J. M. Bakker-Woudenberg, C. Kluft, and G. Storm. 1993. Specific targeting with poly(ethylene glycol)-modified liposomes: coupling of homing devices to the ends of the polymeric chains combines effective target binding with long circulation times. *Biochim. Biophys. Acta.* 1149:180–184.

Boivin, S., A. Chettouf, P. Hemery, and S. Boileau. 1983. Chemical modification of poly(vinyl chloroformate) and of its copolymers using phase transfer catalysis. *Polym. Bull.* 9:114–120.

Boivin, S., P. Hemery, and S. Boileau. 1985. Polymérisation du chloroformiate de vinyle et de ses dérivés. *Can. J. Chem.* 63:1337–1343.

Boivin, S., P. Hemery, and S. Boileau. 1988. Chemical modification of poly(vinyl chloroformate) by phenol using phase-transfer catalysis. *In* Chemical Reactions on Polymers. J. L. Benham and J. F. Kinstle, editors. American Chemical Society, Washington, DC. 37–45.

Candau, S. J. 1986. Light scattering. *In* Surfactant Solutions. R. Zana, editor. Marcel Dekker, New York. 155–160.

Carter, K. C., A. J. Baillie, J. Alexander, and T. F. Dolan. 1988. The therapeutic effect of sodium stibogluconate in Balb/c mice infected with *Leishmania donovani* is organ-dependent. *J. Pharm. Pharmacol.* 40: 370–373.

Chopineau, J., S. Lesieur, and M. Ollivon. 1994. Vesicle formation by enzymatic process. *J. Am. Chem. Soc.* 116:11582–11583.

Corti, M. 1985. Physics of Amphiphiles: Micelles, Vesicles and Microemulsions. Elsevier Publishing Company, New York.

de Gennes, P. G. 1980. Conformations of polymers attached to an interface. *Macromolecules.* 13:1069–1075.

Dubochet, J., M. Adrian, J. J. Chang, J. C. Homo, J. Lepault, A. W. McDowall, and P. Schultz. 1988. Cryo-electron microscopy of vitrified specimens. *Q. Rev. Biophys.* 21:129–228.

Edwards, K., M. Johnsson, G. Karlsson, and M. Silvander. 1997. Effect of PEG-phospholipids on aggregate structure in preparations of small unilamellar liposomes. *Biophys. J.* 73:258–266.

Erdogan, S., A. Y. Özer, M. T. Ercan, M. Eryilmaz, and A. A. Hincal. 1996. In vivo studies on iopromide radiopaque niosomes. *Scientific and Technical Pharmacy. Pharmaceutical Sciences*. 6:87–93.

Florence, A. T. 1993. Nonionic surfactant vesicles: preparation and characterization. *In* Liposome Technology. G. Gregoriadis, editor. CRC Press, Boca Raton, FL. 157–176.

Florence, A. T., and A. J. Baillie. 1989. Non-ionic surfactant vesicles, alternatives to liposomes in drug delivery? *In* Novel Drug Delivery and Its Therapeutic Application. L. F. Prescott and W. S. Nimmo, editors. John Wiley and Sons, New York. 281–296.

Handjani-Vila, R. M., A. Ribier, A. Rondot, and G. Vanlerberghe. 1979. Dispersions of lamellar phases of non-ionic lipids in cosmetic products. *Int. J. Cosmetic Sci.* 1:303–314.

Handjani-Vila, R. M., A. Ribier, and G. Vanlerberghe. 1982. Les niosomes. *in* Les liposomes. Lavoisier, Paris. 297–313.

Hristova, K., A. Kenworthy, and T. J. McIntosh. 1995. Effect of bilayer composition on the phase behavior of liposomal suspensions containing poly(ethylene glycol)-lipids. *Macromolecules.* 28:7693–7699.

Hristova, K., and D. Needham. 1994. The influence of polymer-grafted lipids on the physical properties of lipid bilayers: a theoretical study. *J. Colloid Interface Sci.* 168:302–314.

Hristova, K., and D. Needham. 1995. Phase behavior of a lipid/polymer-lipid mixture in aqueous medium. *Macromolecules.* 28:991–1002.

Hunter, C. A., T. F. Dolan, G. H. Coombs, and A. J. Baillie. 1988. Vesicular systems (niosomes and liposomes) for delivery of sodium stibogluconate in experimental murine visceral leishmaniasis. *J. Pharm. Pharmacol.* 40:161–165.

Ishiwata, H., A. Vertut-Doï, T. Hirose, and K. Miyajima. 1995. Physical-chemistry characteristics and biodistribution of poly(ethylene glycol)-coated liposomes using poly(oxyethylene) cholesteryl ether. *Chem. Pharm. Bull.* 43:1005–1011.

Janzen, J., X. Song, and D. E. Brooks. 1996. Interfacial thickness of liposomes containing poly(ethylene glycol)-cholesterol from electrophoresis. *Biophys. J.* 70:313–320.

Kenworthy, A., K. Hristova, D. Needham, and T. J. McIntosh. 1995a. Range and magnitude of the steric pressure between bilayers containing phospholipids with covalently attached poly(ethylene glycol). *Biophys. J.* 68:1921–1936.

Kenworthy, A., S. A. Simon, and T. J. McIntosh. 1995b. Structure and phase behavior of lipid suspensions containing phospholipids with covalently attached poly(ethylene glycol). *Biophys. J.* 68:1903–1920.

Kerr, D. J., A. Rogerson, G. J. Morrison, A. T. Florence, and S. B. Kaye. 1988. Antitumor activity and pharmacokinetics of niosome encapsulated adriamycin in monolayer, spheroid and xenograft. *Br. J. Cancer.* 58: 432–436.

Kirpotin, D., K. Hong, N. Mullah, D. Papahadjopoulos, and S. Zalipsky. 1996. Liposomes with detachable polymer coating: destabilization and fusion of dioleoylphosphatidylethanolamine vesicles triggered by cleavage of surface-grafted poly(ethylene glycol). *FEBS Lett.* 388:115–118.

Kuhl, T. L., D. E. Leckband, D. D. Lasic, and J. N. Israelachvili. 1994. Modulation of the interaction forces between bilayers exposing short-chained ethylene oxide headgroups. *Biophys. J.* 66:1479–1488.

Lasic, D. D. 1994. Sterically stabilized vesicles. *Angew. Chem. Int. Ed. Engl.* 33:1685–1698.

Lasic, D. D. 1996. Doxorubicin in sterically stabilized liposomes. *Nature.* 380:561–562.

Lasic, D. D., and D. Needham. 1995. The "stealth"liposome: a prototypical biomaterial. *Chem. Rev.* 95:2601–2628.

Lasic, D. D., M. C. Woodle, F. Martin, and T. Valentincic. 1991. Phase behavior of "stealth-lipid"-lecithin mixtures. *Period. Biol.* 93:287–290.

Lesieur, S., C. Grabielle-Madelmont, M. T. Paternostre, J. M. Moreau, R. M. Handjani-Vila, and M. Ollivon. 1990. Action of octyl glucoside on non-ionic monoalkyl amphiphile-cholesterol vesicles: study of the solubilization mechanism. *Chem. Phys. Lipids.* 56:109–121.

Lesieur, S., C. Grabielle-Madelmont, M. Paternostre, and M. Ollivon. 1993. Study of size distribution and stability of liposomes by high performance gel exclusion chromatography. *Chem. Phys. Lipids.* 64: 57–82.

Mazer, N. A., G. B. Benedek, and M. C. Carey. 1990. Quasielastic light scattering studies of aqueous biliary lipids systems, mixed micelle formation in bile salt-lecithin solutions. *Biochemistry.* 19:601–615.

McMullen, T. P., and R. N. McElhaney. 1996. Physical studies of cholesterol-phospholipid interactions. *Curr. Opin. Colloid Interface Sci.* 1:83–90.

Nadeau, H. G. A. S. 1967. Instrumental methods of analysis. *In* Nonionic Surfactant. M. J. Schick, editor. Marcel Dekker, New York. 860–892.

Nallet, F., R. Laversanne, and D. Roux. 1993. Modelling X-ray or neutron scattering spectra of lyotropic lamellar phases: interplay between form and structure factors. *J. Phys. II France.* 3:487–502.

Needham, D., K. Hristova, T. J. McIntosh, M. Dewhirst, N. Wu, and D. D. Lasic. 1992. Polymer-grafted liposomes: physical basis for the "stealth" property. *J. Liposome Res.* 2:411–430.

Needham, D., T. J. McIntosh, and D. D. Lasic. 1992. Repulsive interactions and mechanical stability of polymer-grafted lipid membranes. *Biochim. Biophys. Acta.* 1108:40–48.

Oku, N., and Y. Namba. 1994. Long-circulating liposomes. *Crit. Rev. Ther. Drug Carrier Syst.* 11:231–270.

Ollivon, M., A. Walter, and R. Blumenthal. 1986. Sizing and separation of liposomes, biological vesicles, and viruses by high-performance liquid chromatography. *Anal. Biochem.* 152:262–274.

Raja Naresh, R. A., and N. Udupa. 1996. Niosome encapsulated bleomycin. *Scientific and Technical Pharmacy. Pharmaceutical Sciences*. 6:61–71.

Rogerson, A., J. Cummings, and A. T. Florence. 1987. Adriamycin-loaded niosomes: drug entrapment, stability and release. *J. Microencapsul.* 4:321–328.

Rogerson, A., J. Cummings, N. Willmott, and A. T. Florence. 1988. The distribution of doxorubicin in mice following administration in niosomes. *J. Pharm. Pharmacol.* 40:337–342.

Sankaram, M. B., and T. E. Thompson. 1990. Modulation of phospholipid acyl chain order by cholesterol. A solid-state ^2H nuclear magnetic resonance study. *Biochemistry.* 29:10676–10684.

Sato, T., and J. Sunamoto. 1993. Site specific liposomes coated with polysaccharides. *In* Liposome Technology. CRC Press, Boca Raton, FL. 179–198.

Schneider, T., A. Sachse, J. Leike, G. Rössling, M. Schmidtgen, M. Drechsler, and M. Brandl. 1996. Surface modification of continuously extruded contrast-carrying liposomes: effect on their physical properties. *Int. J. Pharm. (Amst.).* 132:9–21.

Seras, M., K. Edwards, M. Almgren, G. Carlson, M. Ollivon, and S. Lesieur. 1996. Solubilization of non-ionic monoalkyl amphiphile-cholesterol vesicles by octyl glucoside: cryo-transmission electron microscopy of the intermediate structures. *Langmuir.* 12:330–336.

Seras, M., J. Gallay, M. Vincent, M. Ollivon, and S. Lesieur. 1994. Micelle-vesicle transition of non-ionic surfactant-cholesterol assemblies induced by octyl glucoside: a time-resolved fluorescence study of dehydroergosterol. *J. Colloid Interface Sci.* 167:159–171.

Seras, M., R. M. Handjani-Vila, M. Ollivon, and S. Lesieur. 1992. Kinetic aspects of the solubilization of non-ionic monoalkyl amphiphile-cholesterol vesicles by octyl glucoside. *Chem. Phys. Lipids.* 63:1–14.

Seras, M., M. Ollivon, K. Edwards, and S. Lesieur. 1993. Reconstitution of non-ionic amphiphile-cholesterol vesicles by dilution of lipids-octyl glucoside mixed micelles. *Chem. Phys. Lipids.* 66:93–109.

Seras-Cansell, M., M. Ollivon, and S. Lesieur. 1996. Generation of non-ionic monoalkyl amphiphile-cholesterol vesicles: evidence of membrane impermeability to octyl glucoside. *Scientific and Technical Pharmacy. Pharmaceutical Sciences*. 6:12–20.

Shimada, K., A. Miyagishima, Y. Sadzuka, Y. Nozawa, Y. Mochizuki, H. Ohshima, and S. Hirota. 1995. Determination of the thickness of the fixed aqueous layer around polyethyleneglycol-coated liposomes. *J. Drug Targeting.* 3:283–289.

Torchilin, V. P. 1996. How do polymers prolong circulation time of liposomes? *J. Liposome Res.* 6:99–116.

Torchilin, V. P., and V. S. Trubetskoy. 1995. Which polymers can make nanoparticulate drug carriers long-circulating? *Adv. Colloid Interface Sci.* 16:141–155.

Trubetskoy, V. S., and V. P. Torchilin. 1995. Use of polyoxyethylene-lipid conjugates as long-circulating carriers for delivery of therapeutic and diagnostic agents. *Adv. Drug Del. Rev.* 16:311–320.

Uchegbu, I. F., J. A. Bouwstra, and A. T. Florence. 1992. Large disk-shaped structures (discomes) in nonionic surfactant vesicle to micelle transitions. *J. Phys. Chem.* 96:10548–10553.

Uchegbu, I. F., and A. T. Florence. 1995. Non-ionic surfactant vesicles (niosomes): physical and pharmaceutical chemistry. *Adv. Colloid Interface Sci.* 58:1–55.

Uchegbu, I. F., D. McCarthy, A. Schätzlein, and A. T. Florence. 1996. Phase transitions in aqueous dispersions of the hexadecyl diglycerol ehter (C16G2) non-ionic surfactant, cholesterol and cholesteryl poly-24-oxyethylene: vesicles, tubules, discomes and micelles. *Scientific and Technical Pharmacy. Pharmceutical Sciences*. 6:33–43.

Uster, P. S., T. M. Allen, B. E. Daniel, C. J. Mendez, M. S. Newman, and G. Z. Zhu. 1996. Insertion of poly(ethylene glycol) derivatized phospholipid into pre-formed liposomes results in prolonged in-vivo circulation time. *FEBS Lett.* 386:243–246.

Vanlerberghe, G., R. M. Handjani-Vila, and A. Ribier. 1978. Les niosomes, une nouvelle famille de vésicules à base d'amphiphiles non ioniques. *In* Physicochimie des composés amphiphiles. Coll. Nat. CNRS. Editions du CNRS. Paris. 303–311.

Vanlerberghe, G., and J. L. Morançais. 1996. Niosomes in perspective. *Scientific and Technical Pharmacy. Pharmaceutical Sciences*. 6:5–11.

Vertut-Doï, A., H. Ishiwata, and K. Miyajima. 1996. Binding and uptake of liposomes containing a poly(ethylene glycol) derivative of cholesterol (stealth liposomes) by the macrophage cell line J774: influence of PEG content and its molecular weight. *Biochim. Biophys. Acta.* 1278:19–28.

Vinson, P. K., Y. Talmon, and A. Walter. 1989. Vesicle-micelle transition of phosphatidylcholine and octyl glucoside elucidated by cryo-transmission electron microscopy. *Biophys. J.* 56:669–681.

Walter, A. 1992. Biomembrane Structure and Function—The State of the Art. Adenine Press, Schenectady, NY.

Wong, M., and T. E. Thompson. 1982. Aggregation of dipalmitoylphosphatidylcholine vesicles. *Biochemistry.* 21:4133–4139.

Woodle, M. C. 1993. Surface-modified liposomes: assessment and characterization for increased stability and prolonged blood circulation. *Chem. Phys. Lipids.* 64:249–262.

Woodle, M. C. 1995. Sterically stabilized liposome therapeutics. *Adv. Drug Del. Rev.* 16:249–265.

Woodle, M. C., L. R. Collins, E. Sponsler, N. Kossovsky, D. Papahadjopoulos, and F. Martin. 1992. Sterically stabilized liposomes. Reduction in electrophoretic mobility but not electrostatic surface potential. *Biophys. J.* 61:902–910.

Woodle, M. C., and D. D. Lasic. 1992. Sterically stabilized liposomes. *Biochim. Biophys. Acta.* 1113:171–199.